Nucleation and Collapse of Scroll Rings in Excitable Media

Tamás Bánsági, Jr. and Oliver Steinbock*

Department of Chemistry and Biochemistry, Florida State University, Tallahassee, Florida 32306-4390, USA

(Received 19 May 2006; published 10 November 2006)

We describe a novel nucleation mechanism of scroll rings in three-dimensional reaction-diffusion systems with anomalous dispersion. The vortices form after the collision of two spherical wave fronts from a third, trailing wave that only partially annihilates in the wake of its predecessor. Depending on the relative positions of the three relevant wave sources, one obtains untwisted or twisted scroll rings. The formation of both vortex structures is demonstrated for a modified Belousov-Zhabotinsky reaction.

DOI: 10.1103/PhysRevLett.97.198301 PACS numbers: 82.40.Ck, 05.45.−a, 87.18.Pj

Spontaneous breaking of symmetries can result in topological defects such as monopoles, domain walls, and vortex lines. The study of these defects has become an integral and important part of modern physics and spans through many, quite diverse research areas. Among the most intriguing examples are vortex structures. They exist in a broad spectrum of different systems such as nonlinear optical devices, superfluids, superconductors, and Bose-Einstein condensates [1,2]. Rotating vortices have also attracted considerable interest in the context of spatially coupled oscillators and excitable media [3] which include cardiac tissue [4], ventricle [5] and hippocampal cultures [6], slime mold colonies [7], egg cells [8], as well as chemical reactions [9]. While our understanding of vortices in oscillatory and excitable systems has increased significantly over the past decade, many questions remain open concerning their three-dimensional analogues [10]. The latter structures are known as scroll waves and are predicted to be the building blocks, or at least relevant features, of turbulent states and various knotted and chain-linked patterns [11]. Moreover, they are believed to cause cardiac arrythmia and sudden cardiac death if present in the human heart [12].

The key toward understanding scroll wave dynamics lies in the shape and the motion of the curves around which wave rotation occurs. In the simplest case, these filaments are straight lines that terminate at the boundaries of the system. For scroll rings, however, the filament is a closed, ring-shaped curve. Both types of filament topologies have been observed in the autocatalytic Belousov-Zhabotinsky (BZ) reaction using optical methods [13,14] and magnetic resonance imaging [15]. Nevertheless, little is known concerning different initiation scenarios of these three-dimensional vortices. It is therefore not surprising that most studies rely on spontaneous nucleation resulting from complex initial conditions created during the mixing of reactant solutions. Scroll waves can also be initiated by briefly introducing a mechanical or photochemical obstacle. This procedure breaks a continuous wave front, thus, seeding a filament along the wave/obstacle line. Last, recent numerical studies suggest that scroll waves can be created through spiral-breakup instabilities in media with externally applied gradients of excitability [16].

We will here demonstrate that the 1,4-cyclohexanedione Belousov-Zhabotinsky (CHD BZ) system [17] is ideally suited for the study of scroll waves. Moreover, qualitative observations (Fig. 1) show surprisingly large vortex densities in certain CHD BZ media. Our experimental studies suggest that these three-dimensional vortices are formed by a novel nucleation mechanism. This mechanism does not rely on external obstacles but is closely related to the system's anomalous dispersion relation. This relation determines that wave velocities decrease with increasing wavelengths. For finite wave packets, this feature yields slow moving frontier pulses that are followed by fast wave fronts. The latter fronts run into the leading pulse, where they vanish in front-to-back collisions. This behavior has

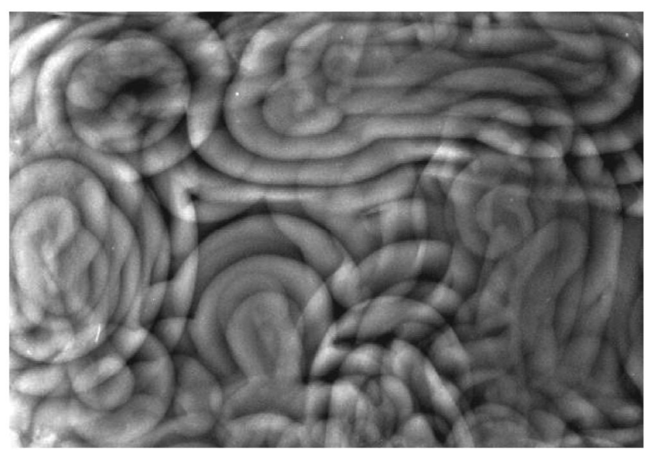

FIG. 1. View through a three-dimensional, highly viscous CHD BZ medium. The snapshot reveals numerous excitation vortices that formed from nearly homogeneous initial conditions and random pacemakers on the walls of a rectangular reaction container. The system depth is 1.9 cm which equals about seven vortex wavelengths. Initial concentrations: $[H_2SO_4] = 0.06$ mol/l, $[NaBrO_3] = 0.18$ mol/l, $[CHD] = 0.19$ mol/l, and $Fe[batho(SO_3)_2]_3^{4-} = 0.475$ mmol/l. Container size: $(4.9 \times 6.0 \times 1.9)$ cm^3. Image area: (4.0×3.0) cm^2.

been coined ''wave merging'' and was reported for the 1,4-cyclohexanedione Belousov-Zhabotinsky (CHD BZ) reaction [17], the catalytic reduction of NO with CO on Pt(100) surfaces [18] and generic models of reaction-diffusion media [19].

We prepare CHD BZ systems by mixing stock solutions of CHD (Aldrich), $NaBrO_3$ (Fluka), and H_2SO_4 (Riedel-de Haën). The complex $Fe[batho(SO_3)_2]_3^{4-}$ is employed as redox catalyst and indicator. By addition of polyacrylamide solution [20], the viscosity of the reaction solution is increased from about 1 to 150 mPa s. This change suppresses undesired hydrodynamic perturbations without using a gel matrix that would prevent stirring and, hence, resetting the system. In contrast to the classic BZ medium, this reaction system also does not produce gaseous products that could compromise the system's spatial homogeneity through bubble formation.

For all experiments with the exception of Fig. 1, the reaction solution is filled into a cylindrical glass cuvette (inner diameter: 3.7 cm). The temperature is kept constant at (21 ± 1) °C. A teflon-coated, magnetic stir bar is modified to fit precisely to the bottom of the cuvette. After preparation, the reaction system remains in a spatially homogeneous, oxidized state for approximately 80 min. At the end of this induction period, we observe the spontaneous formation of various wave patterns. These patterns are erased by briefly stirring the solution, which yields a spatially homogeneous, chemically reduced, and dynamically excitable medium for further, controlled manipulation.

Wave patterns are monitored and analyzed using optical tomography. The samples are illuminated with white light and rotated at a constant period of 4.9 s. Transmission images of the rotating sample are recorded using a charge-coupled-device camera at a rate of 12.5 frames/s. Considering the wave velocity of 0.045 mm/s and the setup's spatial resolution of 0.05 mm/pixel, we find that the wave pattern progresses only slightly (4 pixels) during a full rotation of the sample cuvette. This feature allows the use of the inverse radon transform to reconstruct three-dimensional concentration fields from series of typically 62 projections. The software used for this analysis has been developed in-house using the Matlab environment. Similar tomographic procedures have been described earlier by Winfree and Müller *et al.* [13,14].

The nucleation mechanism requires two pointlike wave sources. In this study, one of these sources is created by gluing a small (~0.1 mm) silver particle onto the stir bar. This particle locally reduces the concentration of an inhibitory bromide ion yielding a periodic pacemaker of excitation waves. The typical period of the pacemaker is approximately 30 s. For the second wave source, we gently touch the solution surface with a thin silver wire for approximately 1 s. This procedure induces a single, downward propagating wave front.

A typical example for the resulting wave pattern is shown in Fig. 2(a). In this transmission snapshot, the silver particle has initiated two upward propagating, half-spherical wave fronts (bright bands in figure). The downward traveling front in the upper portion of the figure was initiated manually. In the course of time, the two outermost wave fronts collide. As expected, the wave fronts fuse while undergoing mutual annihilation. This process yields a single, hourglass-shaped front [see Fig. 2(b)]. In the wake of this front, a trailing pulse vanishes in a front-to-back collision. We reemphasize that this behavior is characteristic for the CHD BZ reaction and dynamically similar systems with anomalous dispersion relations that give rise to ''wave merging''. More precisely, the low-wavelength limit of such dispersion relations corresponds to wave velocities that are larger than the velocity of the solitary pulse (for more details see ref. [17]).

The specific geometry created in the wave collisions induces the formation of a scroll ring. As shown Figs. 2(c)–2(f), the trailing wave front does not vanish within the central gap of the outer front. The resulting front segment has initially the shape of a spherical cap, but its boundary quickly curls up to induce the circular filament of the newly formed single vortex ring. The main steps of this process are also shown in Figs. 2(g)–2(j) which present

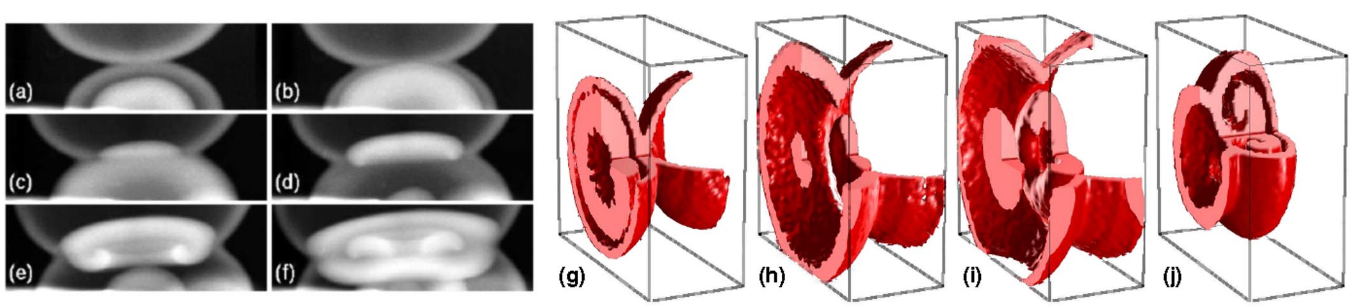

FIG. 2 (color online). Nucleation of untwisted scroll rings in the CHD BZ reaction. (a)–(f) Sequence of snapshots through the three-dimensional system. Image area: (17.0×5.6) mm^2. Time between frames: 20 s. (g)–(j) Tomographically reconstructed concentration fields from a different experimental run. The upper right quarter of each box is removed to reveal details of the wave structure. Time between frames: 30, 15, and 30 s. Size of the boxes: $(21.5 \times 9.8 \times 21.5)$ mm^3. The initial concentration, viscosity, and temperature are the same as in Fig. 1 but a cylindrical container is used.

three-dimensional reconstructions of the wave pattern. Notice that the bottom of the snapshots in Figs. 2(a)–2(f) correspond to the left anterior surfaces in Figs. 2(g)–2(j).

The vortex structure shown in Fig. 2 is phase synchronized along its circular filament and hence untwisted. This absence of any phase difference in spiral rotation is the result of the axially symmetric structure nucleating the scroll ring. Figure 3 demonstrates that this symmetry is lost if, during the nucleation process, the trailing wave front is triggered at a slightly different position. In our experiments, this translation is accomplished by slightly rotating the stir bar in the reaction system with an external magnet. This rotation shifts the off-center mounted silver particle to the desired new position. The three-dimensional reconstruction in Fig. 3(a) shows a typical example for the resulting wave pattern. The two wave fronts on the left are triggered from points separated by approximately 1 mm. Figure 3(b) illustrates the resulting vortex and an additional wave front on the left. The scroll ring is twisted with an initial phase difference (about 180° in Fig. 3) that depends on the time elapsed between the three front nucleations and the specific dispersion relation of the system. Time-resolved measurements indicate that the associated torsion disappears during vortex rotation, thus, untwisting the wave structure. Moreover, at all times the pattern remains symmetric with respect to a mirror plane defined by the three relevant pacemaker locations. Notice that the reconstructions in Fig. 3 show only the posterior half of the structure.

The nucleation examples in Figs. 2 and 3 share certain similarities with the wave-induced formation of spiral waves in two-dimensional CHD BZ media [21]. In the latter situation, the collision of circular, merging wave fronts creates a pair of counterrotating spirals and numerous nonrotating defects in the wake of the leading frontier pulse. As we reported earlier [21], the rotation centers of the spiral pair remain stationary. In the three-dimensional medium, however, the scroll ring's filament is not stationary. Figure 4(a) illustrates the filament motion for a representative experiment. The plot shows three consecutive filament reconstructions of an untwisted vortex revealing that (i) the filament remains circular, (ii) that the radius of the filament decreases in the course of time and (iii) that the center of the filament moves in a direction perpendicular to the filament plane. The drift occurs in the direction with which the wave front passes through the filament loop. Moreover, the shrinkage of the filament finally induces the annihilation of the vortex structure. In the example of Fig. 4, the total time elapsed between vortex birth and death is about 700 s, which corresponds to about 17 rotation periods of the wave pattern.

Figure 4(b) shows a quantitative analysis of the filament radius R (open squares) and its vertical drift coordinate z (open circles). The time $t = 0$ corresponds to the situation immediately after the wave-induced initiation of the scroll ring for which z is set to zero. The data reveal that filament shrinkage and translation become more pronounced over the lifetime of the vortex. Earlier theoretical analyses [22] predicted that untwisted scroll rings obey

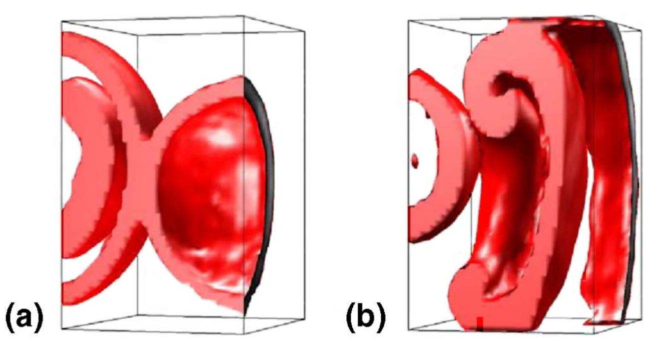

FIG. 3 (color online). Tomographically reconstructed three-dimensional snapshots illustrating the formation of a twisted scroll ring. The anterior half of each box is removed to reveal the vortex structure. Time between frames: 75 s. Initial concentration, viscosity, and temperature are the same as in Fig. 1. Size of the boxes: $(7.3 \times 8.2 \times 11.7)$ mm^3.

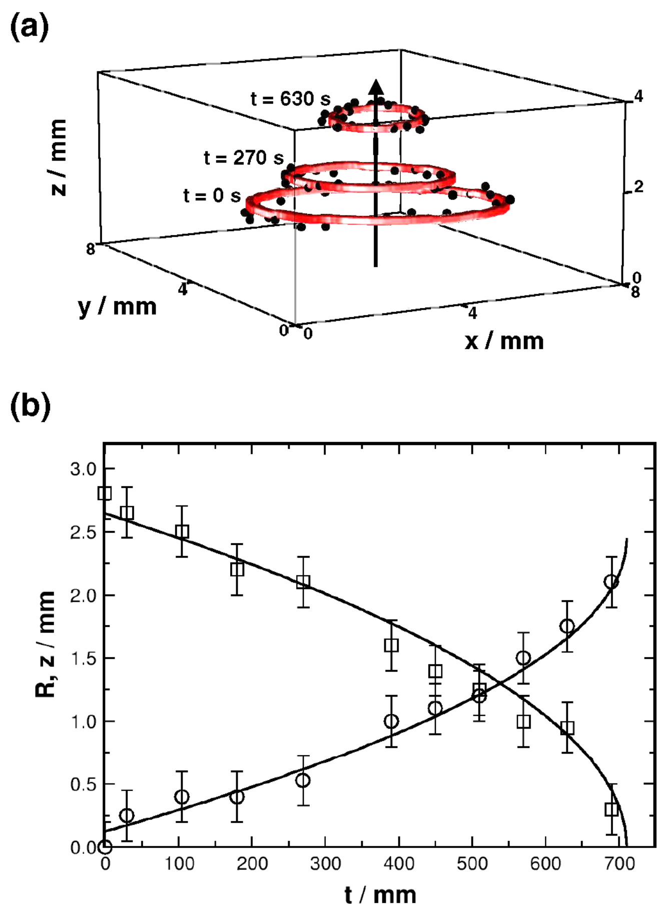

FIG. 4 (color online). Collapse and drift of an untwisted scroll ring. (a) Three reconstructed snapshots of a shrinking vortex filament. (b) Filament radius R (open squares) and vertical position z (open circles) as a function of time. Theoretical fits based on Eqs. (2) are represented by solid lines. Initial concentration, viscosity, and temperature are the same as in Fig. 1.

$$\frac{dR}{dt} = -\frac{\alpha}{R}, \qquad \frac{dz}{dt} = \frac{\beta}{R}, \tag{1}$$

where α denotes the filament tension and β characterizes the rate of vertical translation. These equations yield

$$R = \sqrt{R_0^2 - 2\alpha t}, \qquad z(t) = z_0 - \frac{\beta}{\alpha} R(t), \tag{2}$$

where R_0 denotes the initial radius of the scroll ring and $z_0 = \frac{\beta}{\alpha} R_0$ is a constant. A least-squares fit of the latter equations yields good agreement between our experimental data and the theoretical predictions. The best fitting curves are shown as solid lines in Fig. 4(b). For the specific set of parameters employed here, we obtain $\alpha = (4.9 \pm 0.3) \times 10^{-5}\ \mathrm{cm}^2/\mathrm{s}$ and $\beta = (4.3 \pm 0.3) \times 10^{-5}\ \mathrm{cm}^2/\mathrm{s}$. To our knowledge, this is the first measurement of β in any excitable system and only the second reported value for the filament tension α. The latter quantity had been estimated by Vinson *et al.* [23] for a different BZ medium as $2 \times 10^{-5}\ \mathrm{cm}^2/\mathrm{s}$.

In conclusion, our study documents a novel type of scroll ring nucleation that should exist in many excitable systems with anomalous dispersion relations including biological media. In the context of our experimental model, this intriguingly simple mechanism also explains the high density of scroll rings that reliably form from nearly homogeneous, initial conditions. Moreover, this type of scroll ring nucleation could prove to be a useful tool for future systematic investigations of these vortices. These investigations should include the systematic exploration of the (α, β)-parameter space and the search for conditions with negative filament tension for which filaments are expected to expand, buckle, and induce turbulent states [24].

This material is based upon work supported by the National Science Foundation under Grant No. 0513912.

---

*Electronic address: steinbck@chem.fsu.edu

[1] M. R. Matthews, B. P. Anderson, P. C. Haljan, D. S. Hall, C. E. Wieman, and E. A. Cornell, Phys. Rev. Lett. **83**, 2498 (1999).

[2] A. S. Desyatnikov, Yu. S. Kivshar, and L. Torner, Prog. Opt. **47**, 291 (2005).

[3] M. C. Cross and P. C. Hohenberg, Rev. Mod. Phys. **65**, 851 (1993); M. C. Cross and P. C. Hohenberg, in *Spatio-Temporal Pattern Formation (With Examples from Physics, Chemistry, and Materials Science)*, edited by C. Walgraef (Springer-Verlag, New York, 1997).

[4] J. M. Davidenko, A. V. Pertsov, R. Salomonsz, W. Baxter, and J. Jalife, Nature (London) **355**, 349 (1992).

[5] S. M. Hwang, K. H. Yea, and K. J. Lee, Phys. Rev. Lett. **92**, 198103 (2004).

[6] M. E. Harris-White, S. A. Zanotti, S. A. Frautschy, and A. C. Charles, J. Neurophysiol. **79**, 1045 (1998).

[7] O. Steinbock, F. Siegert, S. C. Müller, and C. Weijer, Proc. Natl. Acad. Sci. U.S.A. **90**, 7332 (1993).

[8] J. Lechleiter, S. Girard, E. Peralta, and D. Clapham, Science **252**, 123 (1991).

[9] S. Jakubith, H. H. Rotermund, W. Engel, A. von Oertzen, and G. Ertl, Phys. Rev. Lett. **65**, 3013 (1990).

[10] A. T. Winfree, Science **181**, 937 (1973); B. J. Welsh, J. Gomatam, and A. E. Burgess, Nature (London) **304**, 611 (1983).

[11] A. T. Winfree, Nature (London) **371**, 233 (1994).

[12] R. H. Clayton, E. A. Zhuchkova, and A. V. Panfilov, Prog. Biophys. Molec. Biol. **90**, 378 (2006).

[13] A. T. Winfree, S. Caudle, G. Chen, P. McGuire, and Z. Szilagyi, Chaos **6**, 617 (1996).

[14] U. Storb, C. R. Neto, M. Bär, and S. C. Müller, Phys. Chem. Chem. Phys. **5**, 2344 (2003).

[15] A. L. Cross, R. L. Armstrong, C. Gobrecht, M. Paton, and C. Ware, Magn. Reson. Imaging **15**, 719 (1997).

[16] C. Wang, S. Wang, C. Zhang, and Q. Ouyang, Phys. Rev. E **72**, 066207 (2005).

[17] C. T. Hamik, N. Manz, and O. Steinbock, J. Phys. Chem. A **105**, 6144 (2001).

[18] J. Christoph, M. Eiswirth, N. Hartmann, R. Imbihl, I. G. Kevrekidis, and M. Bär, Phys. Rev. Lett. **82**, 1586 (1999).

[19] C. Elphick, E. Meron, and E. A. Spiegel, Phys. Rev. Lett. **61**, 496 (1988).

[20] Polyacrylamide solution prepared as in T. Rica, D. Horváth, and Á. Tóth, Chem. Phys. Lett. **408**, 422 (2005).

[21] N. Manz, C. T. Hamik, and O. Steinbock, Phys. Rev. Lett. **92**, 248301 (2004).

[22] J. P. Keener, Physica D (Amsterdam) **31**, 269 (1988).

[23] M. Vinson, S. Mironov, S. Mulvey, and A. Pertsov, Nature (London) **386**, 477 (1997).

[24] S. Alonso, F. Sagues, and A. S. Mikhailov, Science **299**, 1722 (2003).